Fourth International Conference on Sustainable Construction Materials and Technologies
http://www.claisse.info/Proceedings.htm

SCMT4
Las Vegas, USA, August 7-11, 2016

Sustainability Effects of Including Concrete Cracking and Healing in Service Life Prediction for Marine Environments

Philip Van den Heede[1a,2a], Bjorn Van Belleghem[1b,2b], Michel De Keersmaecker[3a], Annemie Adriaens[3b], and Nele De Belie[1c]

[1]Magnel Laboratory for Concrete Research, Ghent University, Technologiepark Zwijnaarde 904, BE-9052 Ghent (Zwijnaarde), BELGIUM.

[2]Strategic Initiative Materials (SIM vzw), project ISHECO within the program 'SHE'.

[3]Department of Analytical Chemistry, Ghent University, Krijgslaan 281 S12, BE-9000 Ghent, BELGIUM.
[1a,2a]Email: <philip.vandenheede@ugent.be>, [1b,2b]Email: <bjorn.vanbelleghem @ugent.be>,
[3a]Email: <michel.dekeersmaecker@ugent.be, [3b]Email: < annemie.adriaens@ugent.be>,
[1c]Email: <nele.debelie@ugent.be>.

ABSTRACT

With today's focus on sustainable design, it is necessary to adequately predict and prolong service life of concrete in marine environments. By introducing self-healing properties, service life extension can be achieved. However, in prediction models, the required concrete mix specific input is usually not available. Moreover, little attention goes to the unavoidable presence of cracks. Finally, autonomous crack healing has almost never been taken into account. In this paper, the relevant model input was estimated from experimental chloride profiles. It enabled an adequate prediction of the chloride-induced steel depassivation period for cracked and uncracked 15% fly ash concrete (8–104 years, respectively). Comparison with self-healing by means of encapsulated polyurethane indicated a 48–76% self-healing efficiency. It could extend the corrosion initiation period to 36–68 years. Being much less subject to time-dependent repair, PU based self-healing concrete has a 77–88% lower environmental impact than traditional (cracked) concrete.

INTRODUCTION

Nowadays, a lot of attention goes to performance based design of steel reinforced concrete structures. Thus, a profound notion of the material's service life is required as the need for rehabilitation actions in time determines the total concrete amount needed and the overall environmental impact [Van den Heede 2014]. A lot of research efforts also go to the development of concrete types with self-healing properties to significantly extend service life [Van Tittelboom 2012, Wang 2013, Snoeck 2015]. The incorporation of encapsulated polyurethane (PU) is seen as a promising way of achieving this goal [Van Belleghem et al. 2015]. The currently available service life prediction models [fib 2006, DuraCrete 2000] are certainly valuable tools in this evaluation process. However, these models still have some shortcomings. Firstly, few of the prescribed parameters are applicable to just any concrete and any now established differentiation between concrete types is either vague or lacks experimental verification. Secondly, the

models assume that marine concrete structures are crack-free or only contain small cracks (width: 0.1 mm) that can heal autogenously [Maes 2015]. Still, larger cracks are usually unavoidable and serve as preferential pathways for corrosion-inducing substances. This paper deals with those problems for a 15% fly ash (FA) concrete designed for marine exposure conditions. Chloride profiling at various exposure times enabled a proper estimation of the chloride surface concentration, the instantaneous reference chloride diffusion coefficient and the ageing exponent in accordance with Visser et al. [2002]. Furthermore, monitoring of the corrosion potential provided more information on the minimum value for the critical chloride concentration. Cracking was accounted for by assuming reduced concrete covers in the prediction model. In addition, the efficiency of incorporating encapsulated PU to extend service life was evaluated. A life cycle assessment (LCA) methodology was adopted to quantify the environmental benefits/burdens involved.

MATERIALS AND METHODS

Concrete Mixture. The studied concrete mixture can be used in exposure class XS2 which corresponds with environments where concrete is permanently submerged in seawater. A FA containing concrete composition conforming to the k-value concept of NBN B15 001 was manufactured. By using the k-value concept, the maximum fly ash-to-binder (FA/B) ratio for a minimum total binder content equaled 15 %. Per m^3 of this concrete, this gives a CEM I 52.5 N content of 317.6 kg and a FA content of 56 kg for the binder fraction. A water content of 153 kg was assumed to achieve the required water-to-binder (W/B) ratio of 0.41 in compliance with the k-value concept. To make sure the concrete was sufficiently workable some polycarboxylic ether-based superplasticizer (dry matter mass percentage: 35%, density at 20 °C: 1100 kg/m^3) needed to be added. The applied dosage was 3.0 ml/kg binder. This resulted in slump class S3. Regarding the inert fraction, the concrete contained 696 kg river sand 0/4, 502 kg gravel 2/8 and 654 kg gravel 8/16 per m^3 of concrete. The 28-day compressive strength class was C40/50.

Self-Healing Mechanism. Some samples were given self-healing properties by incorporating cylindrical borosilicate glass capsules (inner diameter: 3.00 mm, outer diameter: 3.35 mm, length: 35 mm) filled with a one component PU cf. Van Tittelboom et al. [2011]. They are characterized by a high brittleness. As such, they break easily upon crack occurrence. The healing agent was a non-commercial PU which was developed within the framework of another research project on self-healing concrete (SHEcon). It can be compared with a typical flexible PU foam of which the precursor essentially consists of methylene diphenyl diisocyanate (MDI) and a polyether polyol. This precursor reacts with water to create the foam that should heal the cracks. The moisture content of the concrete itself counts as the main water source.

Curing, Sample Preparation, Cracking and Healing. Chloride diffusion tests cf. NT Build 443 were performed on three cylinders (n = 3, diameter: 100 mm, height: 50 mm) per testing age. The uncracked samples were obtained from concrete cubes (side: 150 mm) that were cured at 20°C and 95% relative humidity until the age of 21 days and then partially coated to ensure a unidirectional chloride ingress later on. The samples containing a standardized artificial crack were cast in cylindrical PVC molds. These cracks were created cf. Mu [2012] by putting thin brass plates with a thickness of 0.3 mm at a depth of 25 mm in the molds just before casting. The plates were carefully removed from the samples after approximately 24 h of curing whereupon the cylinders were demolded. From then on, they were stored again under the same conditions until the age of 21 days to apply the coating. The cracked samples with self-healing properties were manufactured in a very similar way. The only difference was that the thin brass plates contained three holes with a 20 mm spacing. The glass capsules containing the PU were put through these holes and fixed with nylon threads to the sides of the molds. After casting the concrete, capsule breakage and crack healing was triggered by pulling out the thin brass plates (cf. Van Belleghem et al. [2015]). This was done only after 28 days, just before the start of the diffusion test. Some uncracked samples were cast in PVC molds as well as reference. For determining the critical chloride concentration

as suggested by RILEM TC CTC 235, three concrete prisms (200×160×140 mm³) with embedded prerusted ribbed rebar (diameter: 10 mm) were cast cf. Van den Heede [2014]. A prismatic portion was sawn out of them to reduce the concrete cover on top of the rebar to 10 mm. In addition, the entire upper surfaces including the concrete surface-rebar interfaces were coated.

Chloride Diffusion Testing. To determine the proper mix specific input parameters for service life prediction of the uncracked concrete, the partially coated cylindrical specimens taken from cubes were stored in an aqueous 33 g/l NaCl solution at 20 °C after 28 days. This concentration corresponds with the normal Cl^- concentration in the North Sea. After 77, 139, 192, 262 and 311 days of exposure each time three cylinders were removed from the solution. Subsequently, 10 concrete powders were collected from each cylinder by grinding material in 2 mm layers parallel to the zone directly around the crack (area: 16×78 mm²). Determination of the total chloride concentration per ground layer of powder consisted of an acid-soluble extraction in a nitric acid solution followed by a potentiometric titration against silver nitrate cf. Mu [2012]. The cracked, healed and uncracked samples cast in PVC molds were subjected to a slightly different diffusion test. After 28 days, the concrete was immersed in an aqueous 165 g/l NaCl solution. Given the much higher chloride concentration of this solution, adequate chloride profiling could already be done after 49 days of exposure.

Chloride Profile Fitting. When assuming constant values for the diffusion coefficient and surface chloride concentration, the chloride ingress can be estimated using the well-known model proposed by Collepardi et al. [1972] which is based on Fick's second law of diffusion (Eq. 1).

$$C(x,t) = C_0 + (C_s - C_0) \cdot \left[1 - \mathrm{erf}\left(\frac{x}{\sqrt{4 \cdot D_{app} \cdot t}} \right) \right] \quad (1)$$

with C(x, t), the chloride concentration at depth x and time t, C_s, the constant surface concentration, (m%/binder), C_0, the initial chloride concentration (m%/binder), D_{app}, the apparent diffusion coefficient (m²/s) and erf(.), the error function. Note that D_{app} represents a time-averaged value over the entire exposure period and not an instantaneous value. Values for C_s and D_{app} can be estimated from Eq. 1 by applying non-linear regression analysis on the experimental chloride profiles, usually with omission of the first layer (0-2 mm). However, Visser et al. [2002] demonstrated that D_{app} changes with exposure time and concluded that this time dependency should be included in the prediction models. According to the same authors, the following model should comply with this requirement for continuous exposure (Eq. 2).

$$C(x,t) = C_0 + (C_s - C_0) \cdot \left[1 - \mathrm{erf}\left(\frac{x}{\sqrt{4 \cdot \frac{D_0}{(1-n)} \left(\frac{t_0}{t} \right)^n \cdot t}} \right) \right] \quad (2)$$

with D_0, reference instantaneous diffusion coefficient (m²/s)) at reference time t_0 which is usually 28 days (= 0.0767 years), n, the ageing exponent (–) and t, the exposure time (s). In this equation there are three unknown variables (C_s, D_0 and n) that need to be optimized using the least-of-squares method. Visser et al. [2002] emphasize the importance of fitting all three variables simultaneously for all chloride profiles, measured at different exposure times. An initial estimation of the diffusion coefficient and surface concentration using Eq. 1 followed by a subsequent fitting of the ageing exponent using an age function, will not result in optimum values for the three variables C_s, D_0 and n at once. Thus, also in this research the very same approach as proposed by Visser et al. [2002] was adopted. The full dataset of all

experimental chloride profiles obtained at the five considered exposure times (77, 139, 192, 262 and 311 days) with three replicates per exposure time was considered as a whole in order to estimate C_s, D_0 and n using Eq. 2.

Critical Chloride Concentration. From 28 days onwards, the corrosion potential E(corr) of the embedded prerusted ribbed rebars was monitored versus saturated Calomel reference electrodes (= SCE) until onset of active corrosion during immersion in 33 g/l aqueous NaCl solution. According to RILEM TC 235 CTC this event is characterized by a sudden drop in E(corr) of at least 150 mV whereafter the potential remains stable at this lower value. The continuous monitoring of E(corr) was done with a PGSTAT 101 potentiostat/galvanostat (Metrohm Autolab). The total chloride concentration near the rebar at the moment of the potential drop, counts as an estimate for the critical chloride concentration.

Self-Healing Efficiency. The effectiveness of crack healing was assessed by comparing the fitted profiles for uncracked, cracked and healed concrete. This fitting was done using Eq. 1. To obtain a good fit for the cracked and healed samples, the average chloride concentration recorded at a depth of 19 mm was set to correspond with the initial chloride concentration C_0 in the model. Obviously, this chloride concentration is not to be attributed to the initial presence of chlorides before exposure. This is rather due to a non-diffusion controlled fast ingress of chlorides through the (partially healed) crack. Nevertheless, this approach was followed anyway to ensure a proper profile fit. Given the above mentioned issues regarding the proper value for C_0, the fitted C_s and D_{app} values for uncracked, cracked and healed concrete cannot really be compared with each other. Instead, the difference in chloride concentration between the cracked and healed samples as well as the difference in chloride concentration between the cracked and the uncracked samples were calculated for each considered depth from the concrete surface. The ratio of the former over the latter difference expressed in percent was then defined as the self-healing efficiency for each 2 mm thick layer in the profile.

SERVICE LIFE PREDICTION

Limit State Function. The limit state function (Eq. 3) used for estimating the time to chloride-induced steel depassivation looks very similar to the model proposed by Visser et al. [2002].

$$C_{crit} = C_0 + (C_s - C_0) \cdot \left[1 - \mathrm{erf}\left(\frac{d}{\sqrt{4 \cdot k_e \cdot \frac{D_0}{1-n} \cdot \left(\frac{t_0}{t} \right)^n \cdot t}} \right) \right] \tag{3}$$

Only difference is that an environmental transfer variable k_e has been added to the model to account for the difference in temperature between the aqueous exposure solution used for the laboratory diffusion tests and seawater. In accordance with fib [2006], an Arrhenius function was used for this purpose (Eq. 4).

$$k_e = \exp\left(b_e \left(\frac{1}{T_{ref}} - \frac{1}{T_{real}} \right) \right) \tag{4}$$

with b_e, a regression variable which follows a normal distribution (= 4800 ± 700 K), T_{ref}, the constant test temperature (= 293 K or 20 °C) and T_{real}, the temperature of the seawater (= 283 K or 10 °C). Apart from that, variable x in Eq. 2 has been replaced with the concrete cover d on top of the reinforcing steel for this

case study. NBN EN 1992-1-1 prescribes a minimum concrete cover of 50 mm for construction class S6 which corresponds with a design service life of 100 years in exposure class XS2. Although strictly specified, the actual value of this cover varies due to the unavoidable inaccuracies that occur in the construction stage. Therefore, this parameter has to be considered as a stochastic variable. As such, a standard deviation of 8 mm on the minimum cover was taken into consideration. The latter value is seen as appropriate for concrete without particular execution requirements [fib 2006]. The probabilistic distribution of the concrete cover was considered lognormal. The presence of cracks in the concrete was accounted for by assuming a reduced concrete cover. For instance, in case of the applied crack depth of 25 mm, the concrete cover at the crack location was reduced to 25 mm. The critical chloride concentration, represented by C_{crit} in Eq. 3, counts as the decisive criterion in the limit state function. Once the chloride concentration at the location of the steel rebar reaches this critical value, onset of active corrosion can start. In this case study, this event is seen as the end of service life.

Calculation Approach. Reliability indices (β) and probabilities of failure (P_f) associated with the limit state function (Eq. 3) were calculated using the First Order Reliability Method (FORM) available in the probabilistic Comrel software. Cf. fib [2006], these parameters need to meet the requirements for the depassivation limit state ($\beta \geq 1.3$ and $P_f \leq 0.10$) to qualify for use in a XS2 environment. Table 1 summarizes the applied distributions and their characterizing parameters for all model input.

Table 1. Default and estimated mixture specific input to the service life prediction model

Variable	Distribution	Mean	Stdv.	Upper boundary	Lower boundary
C_0 (m%/binder)	Constant	0.00	–	–	–
d (mm)	Lognormal	25/37/44/50	8	–	–
b_e (K)	Normal	4800	700	–	–
T_{ref} (K)	Constant	293	–	–	–
T_{real} (K)	Normal	283	5	–	–
t_0 (years)	Constant	0.0767 (28 d)	–	–	–
C_s (m%/binder)	Normal	3.42	0.05	–	–
D_0 (mm²/years)	Normal	89	3	–	–
n (–)	Beta	0.33	0.04	0.00	1.00
C_{crit} (m%/binder)	Beta	1.22	0.02	0.00	2.00

LIFE CYCLE ASSESSMENT

In compliance with ISO 14040, the LCA consisted of four major steps: the definition of goal and scope, the inventory analysis, the impact analysis and the interpretation.

Definition of Goal and Scope. This LCA was conducted to quantify the reduction in environmental impact that could be achieved by using the proposed PU based self-healing concrete instead of a traditional concrete in a submerged marine environment. To do this correctly, the LCA study takes into account the difference in service life between traditional (cracked) concrete and the same concrete with self-healing properties. Therefore, the required concrete volume per unit of service life was chosen as functional unit (FU). This was done by dividing the 1 m³ concrete volume by the service life.

Inventory Analysis. Per concrete constituent, the necessary inventory data were collected from the Ecoinvent database [2007]. Their proper short descriptions as mentioned in the database are the following: sand 0/4: 'Sand, at mine/CH U', gravel 2/8 and 8/16: 'Gravel, round, at mine/CH U', CEM I 52.5 N: 'Portland cement, strength class Z 52.5, at plant/CH U', FA: partially contains: 'Electricity, hard

coal, at power plant/BE U', through economic allocation, glass capsule: 'Glass tube, borosilicate, at plant/DE U', PU healing agent: 'Polyurethane, flexible foam, at plant/RER U' (modified).

For the allocation of impacts attributed to the industrial by-product FA, the economic allocation coefficient as proposed by Chen et al. [2010] was applied. This is 1.0% of the impact of the coal fired electricity production corresponding with the production of 1 kg FA. Superplasticizer inventory data were obtained from an environmental declaration published by the EFCA [2006]. The transport of each constituent to the concrete plant was not incorporated in the LCA since its environmental impact is always very case specific. The impacts related with the production process at a concrete plant were included by the partial assignment of the following life cycle inventory (LCI) from Ecoinvent to each concrete composition: 'Concrete, normal at plant/CH U'. It comprises the whole process of producing 1 m^3 of ready-mixed concrete, including all internal processes (transport, wastewater treatment, etc.) and infrastructure, and this for a traditional concrete composition which is also accounted for in the LCI. By removing the original concrete constituents and their transport from this inventory, a new LCI is obtained that simply represents the concrete production in general, without any link with a predefined concrete.

As indicated above, the existing LCI for PU flexible foam was somewhat modified in order to make it more representative for the PU that was used in this research. One important change relates to the fact that the toluene diisocyanate (TDI) needed to be replaced with methylene diphenyl diisocyanate (MDI). Another distinct modification was the removal of the water for reaction with the PU precursor from the LCI, as this water is being provided by the moisture content of the concrete. The PMMA sealant that was used to close the glass tubes once filled with PU was so small that this component could be omitted from the LCI. It was assumed that a concrete volume of 1 m^3 contains 7500 capsules with PU. With this dosage, they would be present in the entire surface area of 1 m^3 of concrete to heal cracks with a depth of 25 mm. The capsule volume was not subtracted from the required concrete amount per m^3 because this would probably cause a strength decrease and an equal strength was assumed for the LCA calculations.

Impact Analysis and Interpretation. With incorporation of encapsulated polymers, it is better to look at more impact category indicators than just the global warming potential. Therefore, the CML-IA (baseline) impact method of the Center of Environmental Science (CML) of Leiden University was used.

RESULTS AND DISCUSSION

Chloride Profile Fitting. The simultaneous fitting of C_s, D_0 and n in accordance with Visser et al. [2002] results in theoretical chloride profiles that match rather well with the experimental data (Figure 1). This seems to be the case for all five exposure times (77, 139, 192, 262 and 311 days). As such, the values for C_s, D_0 and n amount to 3.42 ± 0.05 m%/binder, 89 ± 3 mm^2/years and 0.33 ± 0.04, respectively (Table 1). For this fit an R^2 value of 0.978 was recorded. When looking at the evolution of the chloride profiles as a function of the exposure time it is clear that the chlorides move inwards. In other words, for a given distance (e.g. 10 mm) from the exposure surface, the chloride concentration is gradually increasing. Thus, it is quite evident that that at certain moment, the zone in direct contact with an embedded rebar will reach the critical chloride concentration that causes breakdown of the protective passivation layer on top of the rebar. More details on the expected value of this critical chloride concentration follow in the next section.

Critical Chloride Concentration. The initial stable E(corr) values recorded after connecting the three specimens to the potentiostats amounted to –203 mV, –94 mV and –111 mV, respectively. As these values are more positive than –250 mV vs. SCE, the criterion for passivated steel cf. Izquierdo et al. [2004] is met. By the time the last series of three cylinders were removed from the 33 g/l aqueous NaCl solution after 311 days of exposure, no sudden potential drop of at least 150 mV had already taken place. This means that the chloride concentration near the embedded rebar of all three samples did not reach the critical value for onset of active corrosion yet. Thus, the E(corr) monitoring campaign is still ongoing for

all of them. Nevertheless, given the concrete cover of 10 mm, one could more or less estimate how high the critical chloride concentration is at least by looking at the chloride profiles that were measured after 311 days of exposure (Figure 1). On average, the total chloride concentration now recorded at a depth of around 10 mm for this exposure time amounted to 1.22 m%/binder. For now, this value, well within the possible 0.10–1.96 m%/binder range for C_{crit} according Angst et al. [2009], has been adopted. In accordance with fib [2006], a beta distribution was adopted for this variable, with a default standard deviation of 0.15 m%/binder, a lower boundary of 0.00 m%/binder and an upper boundary of 2.00 m%/binder (Table 1). Evidently, this preliminary value of 1.22 m%/binder should be updated as soon as the drop in E(corr) is detected and the actual, higher C_{crit} value for this concrete type can be measured.

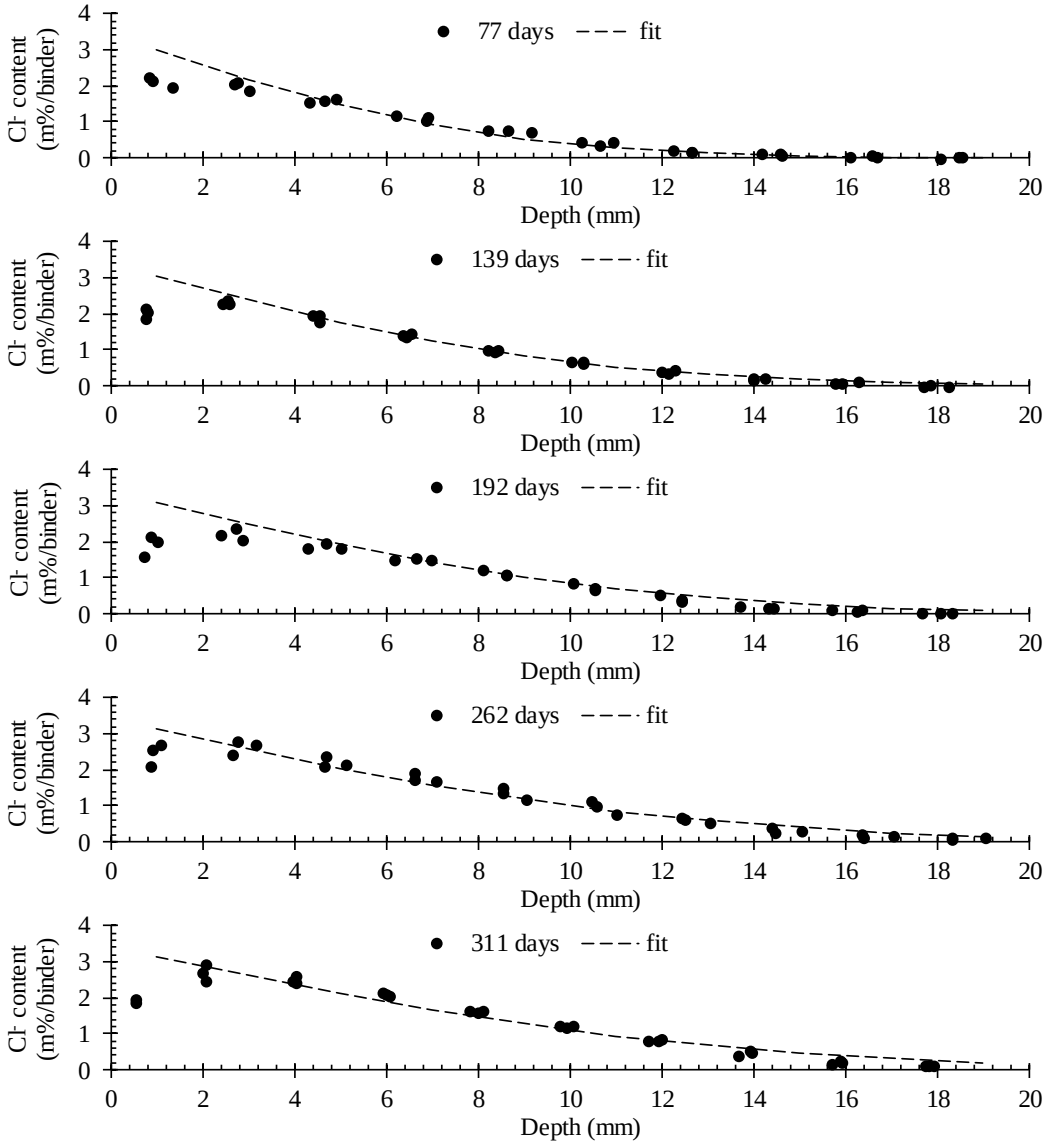

Figure 1. Experimental & fitted choride profiles for uncracked concrete after 77, 139, 192, 262 and 311 days of exposure in an aqueous 33 g/l NaCl solution

Self-Healing Efficiency. The PU healing agent was quite effective in reducing the chloride ingress at the crack location (Figure 2). Still, a 100% crack healing cannot be achieved yet. The fitted chloride profile of

the healed sample does not completely coincide with the profile of the uncracked reference sample. When calculating the self-healing efficiency for each layer in the profiles, the values obtained range between 48–76%. The lower values for the self-healing efficiency were especially recorded in between 0–7 mm from the exposure surface. At higher depths, a more profound healing seems to have taken place. For service life prediction, the original intended concrete cover of 50 mm cannot be assumed since the concrete is not completely behaving as uncracked. Considering the same reduced concrete cover of 25 mm (50 mm concrete cover – 25 mm crack depth) as for the cracked sample may be a bit drastic as the chloride ingress for the samples with self-healing properties had decreased significantly after all. In this theoretical case study, an appropriate range for the reduced concrete cover of the self-healing concrete was calculated by subtracting the complement of the self-healing efficiency multiplied with the 25 mm crack depth from the 50 mm concrete cover. This was done twice. The minimum and maximum recorded self-healing efficiency for the layers were once considered in this preliminary calculation. The resulting reduced concrete covers for service life prediction amounted to 37 and 44 mm, respectively (Table 1).

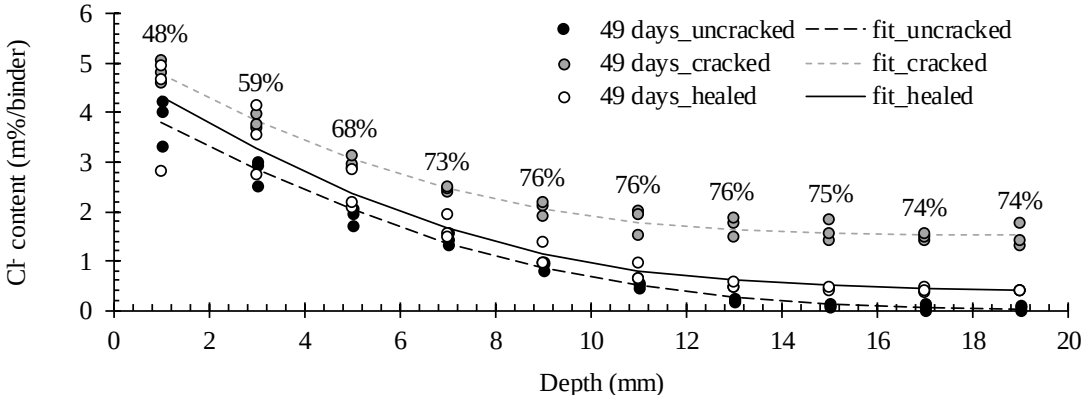

Figure 2. Experimental & fitted choride profiles for cracked, healed and uncracked concrete after 49 days of exposure in an aqueous 165 g/l NaCl solution

Service Life Prediction. In literature, service life prediction models usually assume that concrete is free of cracks when the crack widths do not exceed the maximum crack width allowed [DuraCrete 2000, fib 2006]. Thus, with crack widths lower than 0.3 mm, which is the criterion imposed by NBN EN 1992-1-1 for traditional steel reinforced concrete, the effect of those cracks on the service life outcome should be negligible. Table 2 shows that this is clearly not the case. For the uncracked concrete it would take no less than 104 years for the steel to depassivate, while this would barely be 8 years in presence of a crack, 0.3 mm wide and with a depth of 25 mm. The service life of cracked concrete can be extended substantially by incorporating encapsulated PU. Depending on whether the minimum or maximum healing efficiency can be assumed, the time to depassivation can be postponed to 36–68 years. With a design service life of 100 years, environmental impacts related to intermediate crack repair could thus be eliminated to a large extent by giving the concrete self-healing properties. To fully benefit from this advantage, the impacts related to the initial production of the self-healing concrete should remain acceptable.

Table 2. Estimated time to steel depassivation for cracked, healed and uncracked concrete

Surface condition	Cracked	Minimum healing	Maximum healing	Uncracked
Time to depassivation (years)	8	36	68	104

Life Cycle Assessment. The incorporation of glass capsules filled with the PU obviously increases the environmental impact of the concrete, and this for all ten baseline impact category indicators (Table 3).

However, these additional impacts seem to be still quite low. Depending on the impact category indicator this increase ranges from 1.0% (abiotic depletion potential) to 4.8% (eutrophication potential). The emission of a substantial extra amount of greenhouse gas emissions, which is mostly focused on in environmental studies, turns out to be far from an issue. The extra emissions with adverse consequences for human toxicity (+ 3.0%), ecotoxicity (+ 3.1–4.3%), photochemical ozone creation (+ 3.2%), acidification (+ 3.2%) and eutrophication (+ 4.8%) are clearly more critical. When also considering the service life performance in the FU for LCA, the extra impacts associated with the encapsulated PU become negligible in comparison with the environmental benefits that can be established by extending the service life of the concrete (Table 3). Even when considering the minimum self-healing efficiency, the impacts would be reduced with no less than 77%. With the maximum self-healing efficiency that could achieved for now, all impact category indicators would be 87–88% lower. If in the future a self-healing efficiency of 100% could be realized somehow, a 92% reduction in overall impact would be possible, if the low-profile impact of the optimized self-healing mechanism itself can be maintained of course.

Table 3. Environmental impact for 1 m³ of concrete with(out) encapsulated PU and for the required concrete volume per unit of service life when cracked, healed and uncracked

Impact category indicator			With PU	Without PU
Abiotic depletion potential (ADP, × 10^{1} MJ fossil fuels)			1.13 (+ 1.0%)	1.12
Global warming potential (GWP, × 10^{2} kg CO_2 eq)			3.00 (+ 1.4%)	2.96
Ozone depletion potential (ODP, × 10^{-6} kg CFC-11 eq)			9.66 (+ 2.7%)	9.41
Human toxicity potential (HTP, × 10^{1} kg 1,4-DB eq)			2.36 (+ 3.0%)	2.29
Freshwater aquatic ecotoxicity potential (FAETP, kg 1,4-DB eq)			6.70 (+ 4.3%)	6.42
Marine aquatic ecotoxicity potential (MAETP, × 10^{5} kg 1,4-DB eq)			5.93 (+ 3.1%)	5.75
Terrestrial ecotoxicity potential (TETP, × 10^{-2} kg 1,4-DB eq)			9.06 (+ 3.8%)	8.73
Photochemical ozone creation potential (POCP, × 10^{-2} kg C_2H_4 eq)			2.05 (+ 3.4%)	1.98
Acidification potential (AP, × 10^{-1} kg SO_2 eq)			5.53 (+ 3.2%)	5.36
Eutrophication potential (EP, × 10^{-1} kg PO_4 eq)			1.54 (+ 4.8%)	1.47
Impact category indicator	Cracked	Minimum healing	Maximum healing	Uncracked
ADP (MJ fossil fuels)	1.40	0.32 (– 77%)	0.17 (– 88%)	0.11 (– 92%)
GWP (× 10^{1} kg CO_2 eq)	3.70	0.84 (– 77%)	0.45 (– 88%)	0.30 (– 92%)
ODP (× 10^{-6} kg CFC-11 eq)	1.18	0.27 (– 77%)	0.14 (– 88%)	0.09 (– 92%)
HTP (kg 1,4-DB eq)	2.87	0.66 (– 77%)	0.35 (– 88%)	0.23 (– 92%)
FAETP (× 10^{-1} kg 1,4-DB eq)	8.03	1.88 (– 77%)	1.01(– 87%)	0.64 (– 92%)
MAETP (× 10^{3} kg 1,4-DB eq)	7.18	1.66 (– 77%)	0.89 (– 88%)	0.57 (– 92%)
TETP (× 10^{-2} kg 1,4-DB eq)	1.09	0.25 (– 77%)	0.14 (– 88%)	0.09 (– 92%)
POCP (× 10^{-3} kg C_2H_4 eq)	2.48	0.57 (– 77%)	0.31 (– 88%)	0.20 (– 92%)
AP (× 10^{-2} kg SO_2 eq)	6.70	1.55 (– 77%)	0.83 (– 88%)	0.54 (– 92%)
EP (× 10^{-2} kg PO_4 eq)	1.84	0.43 (– 77%)	0.23 (– 87%)	0.15 (– 92%)

CONCLUSION

Comparison of chloride profiles for uncracked concrete and concrete containing an artificial crack, 0.3 mm wide and 25 mm deep, indicates a much higher chloride ingress for the latter. As concrete is almost never free of cracks – a crack width of 0.3 mm is actually allowed according to the Eurocode – their presence should somehow be accounted for when assessing service life using currently available prediction models for chloride-induced depassivation of embedded reinforcing steel. With an experimentally estimated chloride surface concentration, instantaneous reference chloride diffusion coefficient, ageing exponent and minimum critical chloride concentration, this timespan should be equal to 8 or 104 years for a cracked and uncracked 15% FA concrete suitable for use in exposure class XS2.

According to first preliminary service life calculations, incorporation of encapsulated PU to ensure autonomous crack healing has a self-healing efficiency of 48–76% which could imply an extension of the corrosion initiation period to 36–68 years in theory. Environmental impacts associated with the required concrete volume per unit of service life are much lower (– 77–88%) for the self-healing concrete than for the more traditional concrete with cracks. The additional impacts necessary to produce the encapsulated PU are rather negligible.

ACKNOWLEDGEMENTS

This research under the program SHE (Engineered Self-Healing materials), project ISHECO (Impact of Self-Healing Engineered materials on steel COrrosion of reinforced concrete) was funded by SIM (Strategic Initiative Materials in Flanders) and IWT (Agency for Innovation by Science and Technology). The financial support from the foundations for this study is gratefully acknowledged.

REFERENCES

Angst, U., et al. (2009). "Critical chloride content in reinforced concrete – A review." *Cem. Concr. Res.*, 39(12), 1122-1138.

Chen, C., et al. (2010). "LCA allocation procedure used as an incitative method for waste recycling: An application to mineral additions in concrete." *Resour. Conserv. Recy.*, 54(12), 1231-1240.

Collepardi, M., et al. (1972). "Penetration of chloride ions into cement pastes and concretes." *J. Am. Cer. Soc.*, 55(10), 534-535.

DuraCrete. (2000). *Probabilistic performance based durability design of concrete structures: General guidelines for durability design and redesign*, CUR, Gouda.

EFCA. (2006). "EFCA Environmental Declaration Superplasticizing Admixures (2006)." *EFCA*, http://www.efca.info/publications.html>(Dec. 9, 2015).

Fib (2006). *Fib Bulletin 34, Model code for service life design*, Fib, Lausanne.

Frischknecht, R., and Jungbluth, N., Eds. (2007) *Overview and methodology, Final report ecoinvent v2.0 No. 1*, Swiss Centre for Life Cycle Inventories, St-Gallen.

Izquierdo, D., et al. (2004). "Potentiostatic determination of chloride threshold values for rebar depassivation, Experimental and statistical study." *Electrochim. Acta*, 49(17-18), 2731-2739.

Maes, M. (2015). *Combined effects of chlorides and sulphates on cracked and self-healing concrete in marine environments*, PhD thesis, Ghent University, Ghent.

Mu, S. (2012). *Chloride penetration and service life prediction of cracked self-compacting concrete*, PhD thesis, Ghent University, Ghent.

Snoeck, D. (2015). *Self-healing and microstructure of cementitious materials with microfibres and superabsorbent polymers*, PhD thesis, Ghent University, Ghent.

Van Belleghem, B., et al. (2015). "Analysis and visualization of water uptake in cracked and healed mortar by water absorption tests and X-ray radiography." *Proceedings of the Fourth International Conference on Concrete Repair, Rehabilitation and Retrofitting (ICCRRR-4)*, 2015, 45-53.

Van den Heede, P. (2014). *Durability and sustainability of concrete with high volumes of fly ash*, PhD thesis, Ghent University, Ghent.

Van Tittelboom, K. (2012). *Self-healing concrete through incorporation of encapsulated bacteria- or polymer based healing agents*, PhD thesis, Ghent University, Ghent.

Van Tittelboom, K., et al. (2011). "Self-healing efficiency of cementitious materials containing tubular capsules filled with healing agent." *Cem. Concr. Compos.*, 33(4), 497-505.

Visser, J.H.M., et al. (2002). "Time dependency of chloride diffusion coefficients in concrete." *Proceedings of the Third International RILEM Workshop on Testing and Modelling the Chloride Ingress into Concrete*, 2002, 423-433.

Wang, J. (2013). *Self-healing concrete by means of immobilized carbonate precipitating bacteria*, PhD thesis, Ghent University, Ghent.